A "Circle Limit III" Calculation

Douglas Dunham
Department of Computer Science
University of Minnesota, Duluth
Duluth, MN 55812-3036, USA
E-mail: ddunham@d.umn.edu
Web Site: http://www.d.umn.edu/~ddunham/

Abstract

M.C. Escher's *Circle Limit III* is usually thought to be the most appealing of his four "Circle Limit" patterns. Two artistic/mathematical questions seem to arise: (1) what angle do the white backbone lines make with the bounding circle, and (2) are other such patterns of fish possible? H.S.M. Coxeter answered the first question and I described a 3-parameter family of possible fish patterns in my 2006 Bridges Conference paper. In this paper, I combine those questions by calculating the intersection angle for any such fish pattern.

1. Introduction

Figure 1 below shows a computer rendition of the Dutch artist M.C. Escher's hyperbolic pattern *Circle Limit III*. Figure 2 shows a fish pattern from the combinatorial family of *Circle Limit III* patterns, but with an angular fish motif in the style of Escher's *Circle Limit I*. In my 2006 Bridges paper [4], I introduced

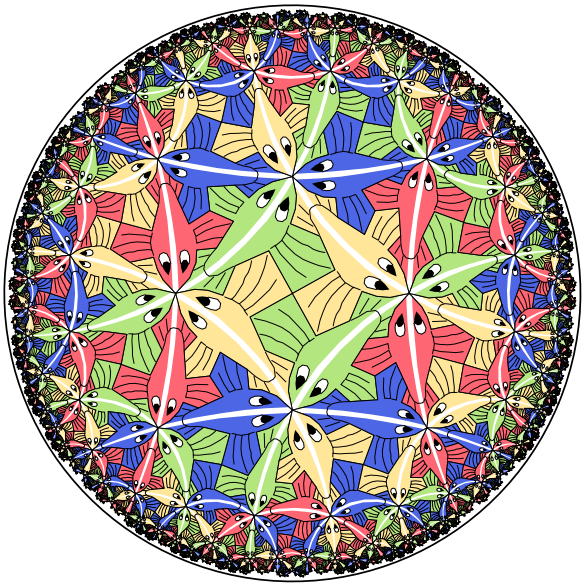

Figure 1: A rendition of Escher's *Circle Limit III*.

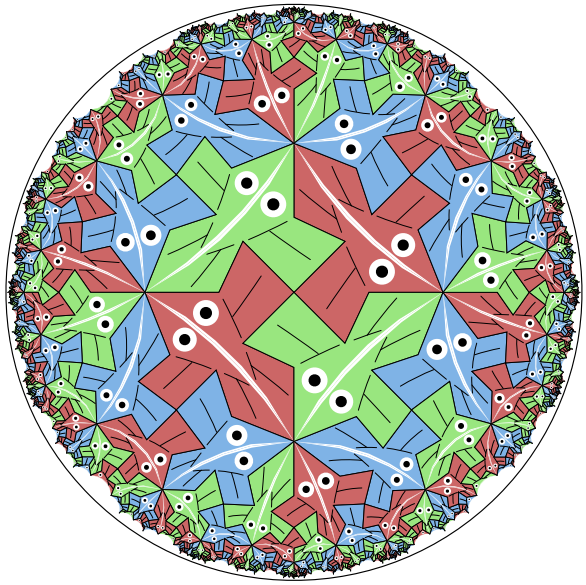

Figure 2: A pattern in the general family of *Circle Limit III*, but in the style of *Circle Limit I*.

the concept of a 3-parameter family of *Circle Limit III* patterns indexed by the numbers $p, q,$ and r of fish meeting at right fin tips, left fin tips, and noses respectively. Such a pattern was denoted by the triple (p, q, r).

So *Circle Limit III* and the pattern of Figure 2 would be named $(4, 3, 3)$ and $(4, 4, 3)$ respectively. Of course r should be odd so that the fish swim head-to-tail, and p, q, and r should all be greater than or equal to 3.

In keeping with the characteristics of *Circle Limit III*, we place some restrictions on the patterns in this family. The first is that right fin tips should be at the center of the bounding circle (for patterns with fin tips at the center). The second condition is that colors of the fish should obey the map-coloring principle: fish that share an edge should be different colors. The fish should also be colored symmetrically and fish along the same "backbone line" should be the same color. Figures 3 and 4 show $(3, 4, 3)$ and $(5, 3, 3)$ patterns. Note the differences between these patterns and *Circle Limit III*. In particular, requiring that a right fin tip be at the center allows us to distinguish between (p, q, r) and (q, p, r) when $p \neq q$.

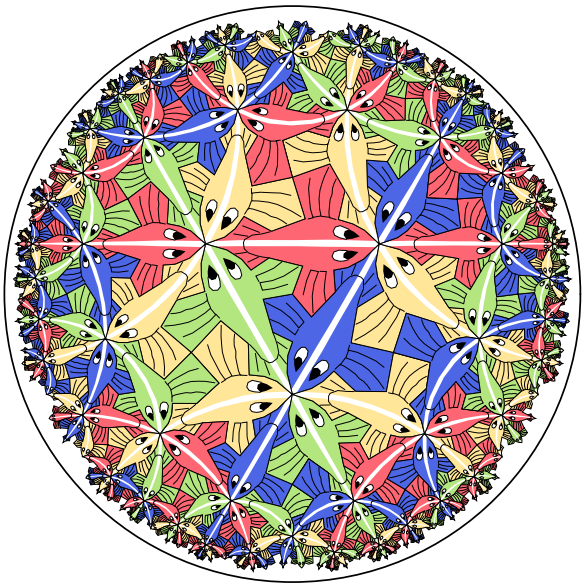

Figure 3: A $(3, 4, 3)$ fish pattern.

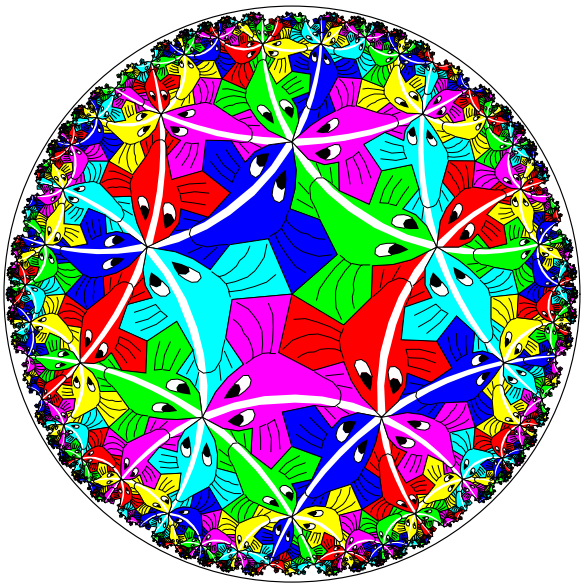

Figure 4: A $(5, 3, 3)$ fish pattern.

As has been recounted before, Escher was inspired to create his "Circle Limit" patterns by a figure showing a tessellation of the hyperbolic plane in one of Canadian mathematician H.S.M. Coxeter's papers. Coxeter in turn, being intrigued by *Circle Limit III*, wrote two papers on the geometry of the backbone lines [2, 3]. In the issue of *The Mathematical Intelligencer* containing Coxeter's second paper, an anonymous editor wrote the following caption for the cover of that issue, which showed *Circle Limit III:*

> Coxeter's enthusiasm for the gift M.C. Escher gave him, a print of Circle Limit III, is understandable. So is his continuing curiosity. See the articles on pp. 35–46. He has not, however said of what general theory this pattern is a special case. Not as yet. [1]

Coxeter did not describe such a general theory, or at least did not publish it. In my 2006 Bridges paper [4], I provided a formula for the angle ω that the backbone lines make with the bounding circle for a $(p, 3, 3)$ pattern. This result generalized the calculations in Coxeter's papers (which only considered $(4, 3, 3)$).

The main goal of this paper is calculate the intersection angle ω between the bounding circle and a backbone line of a general (p, q, r) pattern (all backbone lines of a pattern make the same angle with the bounding circle). First we review some hyperbolic geometry that is used in the calculation. Then we proceed through the calculation, list some results and show a couple of new patterns. Finally, we indicate directions of further research.

2. Hyperbolic Geometry

Escher's "Circle Limit" patterns can be interpreted as repeating patterns of the hyperbolic plane, which is often useful in analyzing their geometry. The hyperbolic plane is a surface of constant negative (Gaussian) curvature and can be considered to be dual to the sphere, which has constant positive curvature. This duality can sometimes be exploited to gain insight into facts about hyperbolic geometry. However, unlike the sphere, the entire hyperbolic plane has no smooth, isometric (distance preserving) embedding in Euclidean 3-space as was proved by David Hilbert in 1901 [6]. Thus, we must rely on Euclidean *models* of hyperbolic geometry in which distance is measured differently and concepts such as hyperbolic lines have interpretations as Euclidean constructs.

We will use two models of hyperbolic geometry: the Poincaré disk model, and the Weierstrass model. In the *Poincaré disk model* the points are just the (Euclidean) points within a Euclidean bounding circle, which we will take to be the unit circle in the xy-plane. Hyperbolic lines are represented by circular arcs orthogonal to the bounding circle (including diameters). For example, the backbone lines lie along hyperbolic lines in Figure 2. The disk model is *conformal*: the hyperbolic measure of an angle is the same as its Euclidean measure. As a consequence, all fish in a "Circle Limit III" pattern have roughly the same Euclidean shape. However equal hyperbolic distances correspond to ever smaller Euclidean distances toward the edge of the disk. So all the fish in *Circle Limit III* patterns are the same (hyperbolic) size. The Poincaré disk model is appealing to artists (and appealed to Escher) since an infinitely repeating pattern could be shown in a bounded area and shapes remained recognizable even for small copies of the motif, due to conformality.

A careful examination of the backbone arcs of the fish in *Circle Limit III* reveals that they are not hyperbolic lines — they make an angle of about 80° with the bounding circle. They are actually *equidistant curves* in hyperbolic geometry: curves at a constant hyperbolic distance from the hyperbolic line with the same endpoints on the bounding circle. For every hyperbolic line and a given distance, there are two equidistant curves, called *branches*, at that distance from the line, one each side of the line. In the Poincaré disk model, those two branches are represented by circular arcs making the same (non-right) angle with the bounding circle on either side of the corresponding hyperbolic line. Equidistant curves are the hyperbolic analogs of small circles in spherical geometry: a small circle of latitude in the northern hemisphere is equidistant from the equator (a great circle or "line" in spherical geometry), and has a second corresponding small circle at the same latitude in the southern hemisphere. Escher used only one branch for fish backbones from each pair of equidistant curves in *Circle Limit III*.

The points in the *Weierstrass model* are the points on the upper sheet of the hyperboloid of two sheets $x^2 + y^2 - z^2 = -1$. The hyperbolic distance between two points $\begin{bmatrix} x_1 \\ y_1 \\ z_1 \end{bmatrix}$ and $\begin{bmatrix} x_2 \\ y_2 \\ z_2 \end{bmatrix}$ is given by: $\cosh^{-1}(z_1 z_2 - x_1 x_2 - y_1 y_2)$. Each hyperbolic line in this geometry is the intersection of a Euclidean plane through the origin with this upper sheet, and so is one branch of a hyperbola. As in spherical geometry, a line can be represented by its *pole*, a 3-vector $\begin{bmatrix} \ell_x \\ \ell_y \\ \ell_z \end{bmatrix}$ on the dual hyperboloid $\ell_x^2 + \ell_y^2 - \ell_x^2 = +1$, so that the line is the set of points satisfying $x\ell_x + y\ell_y + z\ell_z = 0$. Again, in analogy to spherical geometry, equidistant curves are represented by $x\ell_x + y\ell_y + z\ell_z = \pm d$, where d is the hyperbolic distance between the equidistant curve and its line. There is a simple relationship between the Weierstrass model and the disk model: "stereographic projection" onto the xy-plane toward the vertex of the lower sheet of the hyperboloid of two sheets, $\begin{bmatrix} 0 \\ 0 \\ -1 \end{bmatrix}$, which is given by the formula: $\begin{bmatrix} x \\ y \\ z \end{bmatrix} \mapsto \begin{bmatrix} x/(1+z) \\ y/(1+z) \\ 0 \end{bmatrix}$.

3. The Calculation of the Intersection Angle ω

The calculation of the angle a backbone line of a (p, q, r) pattern makes with the bounding circle proceeds through several steps. We first use a hyperbolic trigonometry formula to locate points on a fundamental region for a fish motif. We note that a fundamental region for a fish can be taken to be a *kite*, a quadrilateral with two opposite angles equal, the angles being $\frac{2\pi}{p}$, $\frac{\pi}{r}$, $\frac{2\pi}{q}$, and $\frac{\pi}{r}$. Such tessellations by kites are shown for the *Circle Limit III* pattern in Figure 5 and for the *Circle Limit III* pattern with a nose/tail point at the origin in Figure 6. Then we use the computed points on the Weierstrass model to find one of the points on the equidistant curve. Finally we project that point back down to the Poincaré disk, and use symmetry and Euclidean geometry to find $\cos\omega$.

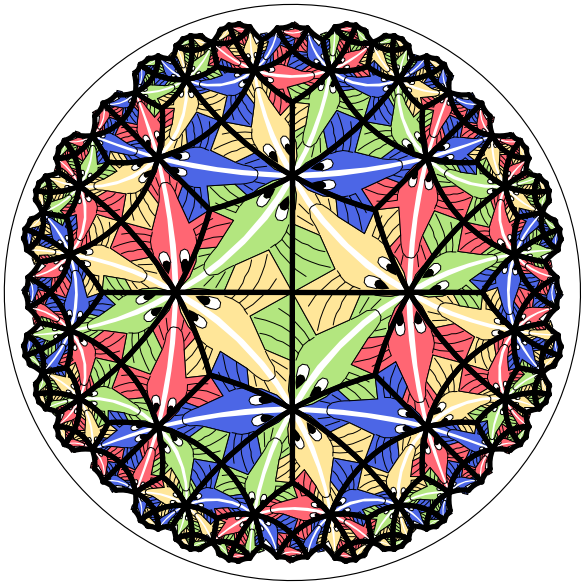

Figure 5: The kite tessellation superimposed on the *Circle Limit III* pattern.

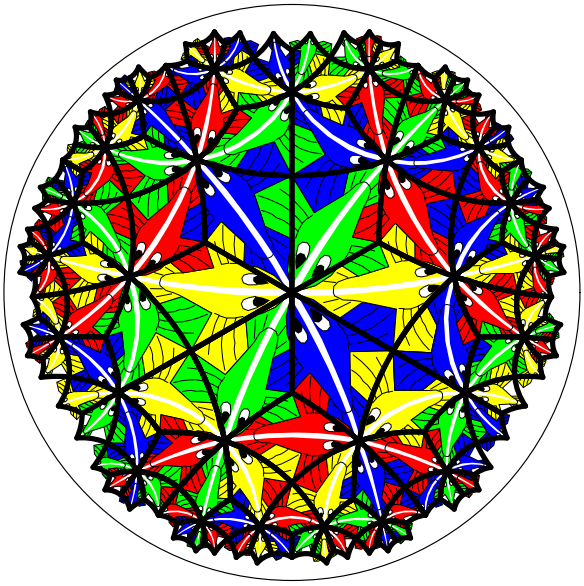

Figure 6: A nose-centered version of Figure 5.

If $p = q$, the backbone lines are hyperbolic lines and $\omega = 90°$. So we can assume $p \neq q$ and, in fact, $p < q$ since the backbone lines of (p, q, r) and (q, p, r) make the same angle. To simplify the calculations, we assume that the tail point of one of the kites is at the origin and the tail angle is bisected by the positive x-axis, with the p-fold point P above the axis and the q-fold point Q below the axis. This configuration is shown in Figure 7, which also shows the hyperbolic line ℓ determined by P and Q, and the equidistant curve through the origin and the other r-fold point, R,of the kite. Figure 8 shows a detailed blowup of the area around the kite.

We start by solving the hyperbolic triangle OPQ for the side lengths d_p and d_q of OP and OQ respectively. Actually, we never need the values of d_p or d_q themselves, only the values of their hyperbolic cosines which, for notational convenience, we will call $coshp$ and $coshq$ (not to be confused with $\cosh(p)$ or $\cosh(q)$, neither of which are useful). Similarly, we let $sinhp = \sqrt{(coshp^2 - 1)}$ and $sinhq = \sqrt{(coshq^2 - 1)}$. Using the conventional notation for a triangle (a, b, and c denote the lengths of the sides opposite angles A, B, and C), one of the standard hyperbolic trigonometry formulas is: $\cosh c = \frac{\cos A \cos B + \cos C}{\sin a \sin b}$ [5, page 406]. We apply that formula to the triangle OPQ, to obtain:

$$coshp = \frac{\cos(\pi/q)\cos(\pi/r) + \cos\pi/p}{\sin(\pi/q)\sin(\pi/r)}, \quad coshq = \frac{\cos(\pi/p)\cos(\pi/r) + \cos\pi/q}{\sin(\pi/p)\sin(\pi/r)} \tag{1}$$

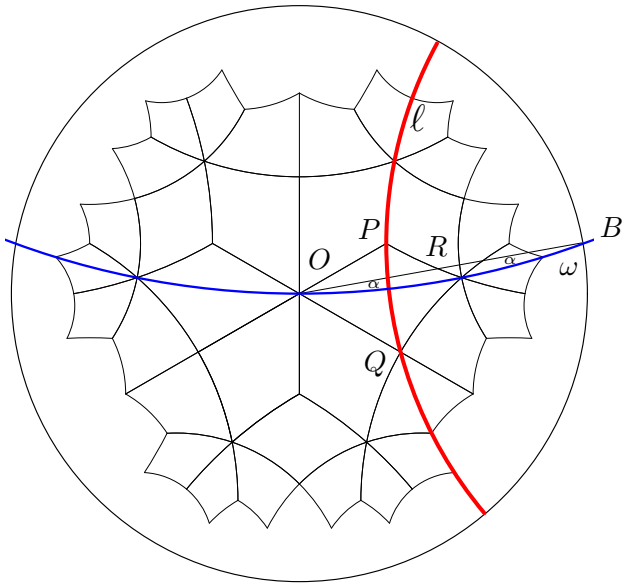

Figure 7: The nose-centered $(4, 3, 3)$ tessellation showing the bisecting line ℓ of the $OPRQ$ kite, the backbone line through O and R, and radius OB.

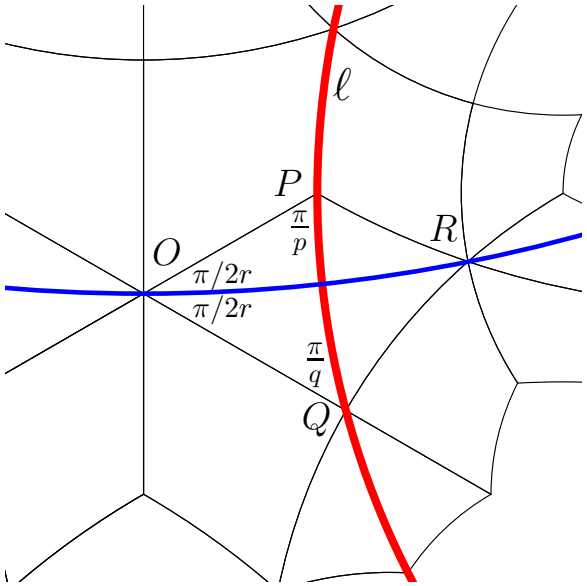

Figure 8: A blowup of the $OPRQ$ kite area of Figure 7.

We can use these values to find the Weierstrass coordinates of P and Q:

$$P = \begin{bmatrix} \cos(\pi/2r)sinhq \\ \sin(\pi/2r)sinhq \\ coshq \end{bmatrix} \quad Q = \begin{bmatrix} \cos(\pi/2r)sinhp \\ -\sin(\pi/2r)sinhp \\ coshp \end{bmatrix} \tag{2}$$

Then the coordinates of the pole of the line ℓ determined by P and Q are given by:

$$\ell = \begin{bmatrix} \ell_x \\ \ell_y \\ \ell_z \end{bmatrix} = \frac{P \times Q}{|P \times Q|} \tag{3}$$

Where the hyperbolic cross-product $P \times Q$ is given by:

$$P \times Q = \begin{bmatrix} P_y Q_z - PzQy \\ P_z Q_x - PxQz \\ -P_x Q_y + PyQx \end{bmatrix} \tag{4}$$

(note the change of sign on the last component), and the norm of a line pole vector V is given by:

$$|V| = \sqrt{(V_x^2 + V_y^2 - V_z^2)} \tag{5}$$

(again note the minus sign before the last term).

Before computing the matrix representing reflection across ℓ, we consider a simpler case. The pole vector representing the hyperbolic line through the point $\begin{bmatrix} \sinh d \\ 0 \\ \cosh d \end{bmatrix}$ and perpendicular to the x-axis is

$\begin{bmatrix} \cosh d \\ 0 \\ \sinh d \end{bmatrix}$, and the matrix ***Ref*** representing reflection of Weierstrass points across that line is given by:

$$Ref = \begin{bmatrix} -\cosh 2d & 0 & \sinh 2d \\ 0 & 1 & 0 \\ -\sinh 2d & 0 & \cosh 2d \end{bmatrix}$$

where d is the the hyperbolic distance from the line (or point) to the origin. Thus reflection across a line whose nearest point to the origin is rotated by angle θ from the x-axis is given by:

$$Rot(\theta)\,Ref\,Rot(-\theta)$$

where, as usual, $Rot(\theta) = \begin{bmatrix} \cos\theta & -\sin\theta & 0 \\ \sin\theta & \cos\theta & 0 \\ 0 & 0 & 1 \end{bmatrix}$. From ℓ we can identify $\sinh d$ as ℓ_z, and $\cosh d$ as $\sqrt{(}\ell_x^2 + \ell_x^2)$, which we denote ρ. Then $\cos\theta = \ell_x/\rho$ and $\sin\theta = \ell_y/\rho$. Thus $\sinh 2d = 2\sinh d\cosh d = 2\rho\ell_z$ and $\cosh 2d = \cosh^2 d + \sinh^2 d = \rho^2 + \ell_z^2$. We can now compute ***Ref***$_\ell$, the matrix for reflection across ℓ as:

$$Ref_\ell = \begin{bmatrix} \frac{\ell_x}{\rho} & -\frac{\ell_y}{\rho} & 0 \\ \frac{\ell_y}{\rho} & \frac{\ell_x}{\rho} & 0 \\ 0 & 0 & 1 \end{bmatrix} \begin{bmatrix} -(\rho^2+\ell_z^2) & 0 & 2\rho\ell_z \\ 0 & 1 & 0 \\ -2\rho\ell_z & 0 & (\rho^2+\ell_z^2) \end{bmatrix} \begin{bmatrix} \frac{\ell_x}{\rho} & \frac{\ell_y}{\rho} & 0 \\ -\frac{\ell_y}{\rho} & \frac{\ell_x}{\rho} & 0 \\ 0 & 0 & 1 \end{bmatrix}$$

Finally we use ***Ref***$_\ell$ to reflect the origin to R since the kite $OPRQ$ is symmetric across ℓ:

$$R = Ref_\ell \begin{bmatrix} 0 \\ 0 \\ 1 \end{bmatrix} = \begin{bmatrix} 2\ell_x\ell_z \\ 2\ell_y\ell_z \\ \rho^2+\ell_z^2 \end{bmatrix} \tag{6}$$

Now we project Weierstrass point R to the Poincaré model:

$$\begin{bmatrix} u \\ v \\ 0 \end{bmatrix} = \begin{bmatrix} \frac{2\ell_x\ell_z}{1+\rho^2+\ell_z^2} \\ \frac{2\ell_y\ell_z}{1+\rho^2+\ell_z^2} \\ 0 \end{bmatrix} \tag{7}$$

The three points $\begin{bmatrix} u \\ v \\ 0 \end{bmatrix}, \begin{bmatrix} -u \\ v \\ 0 \end{bmatrix}$, and the origin determine the (equidistant curve) circle centered at $w = (u^2+v^2)/2v$ on the y-axis, as found by simple geometry. By easy algebra, we find the y-coordinate of the intersection points of this circle, $x^2 + (y-w)^2 = w^2$, with the unit circle to be $y_{int} = 1/2w = v/(u^2+v^2)$. As in Figure 7, let B denote the right-hand intersection point. Then the central angle, α, made by the radius OB with the x-axis is the complement of ω, the angle of intersection of the equidistant curve with the bounding circle, as shown in Figure 7. This can be seen since the equidistant circle is symmetric across the perpendicular bisector of OB. Thus $y_{int} = \sin\alpha = \cos\omega$, so that

$$\cos\omega = y_{int} = v/(u^2+v^2) \tag{8}$$

which is the desired result.

4. Results

The above calculations for $\cos\omega$ have been programmed and have been compared with the values given by the formula $\cos\omega = \frac{1}{2}\sqrt{1 - 3/4\cos^2(\frac{\pi}{2p})}$ given in my 2006 Bridges paper for $(p, 3, 3)$ patterns [4]. This was done for $p = 4, 5, \ldots, 9, 10, 100$, and 1000. In each case the values agreed to within 12 or 13 decimal places (about the limit of double precision on our computers, given roundoff errors in the calculations). Also, a program was designed to draw one of the equidistant curves on a kite tessellation based on a (p, q, r) pattern. In each case we tested, the equidistant curve seemed to pass through the appropriate vertices, as is shown for the particular cases $(3, 4, 5)$ and $(4, 5, 3)$ in Figures 9 and 10 respectively.

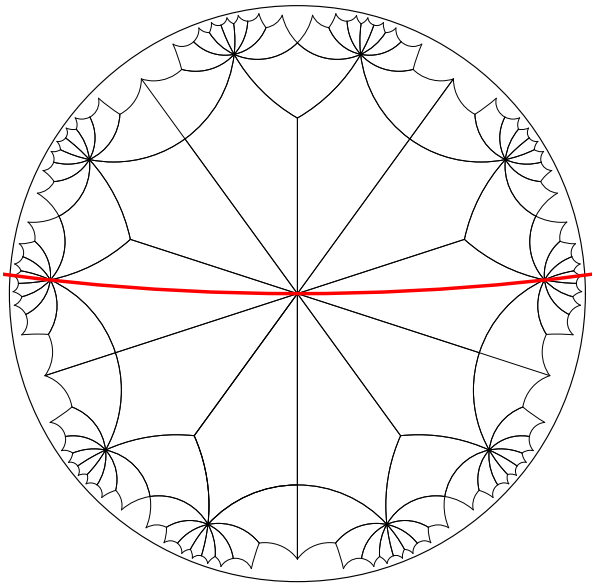

Figure 9: The kite tessellation and a backbone line equidistant curve for a $(3, 4, 5)$ pattern.

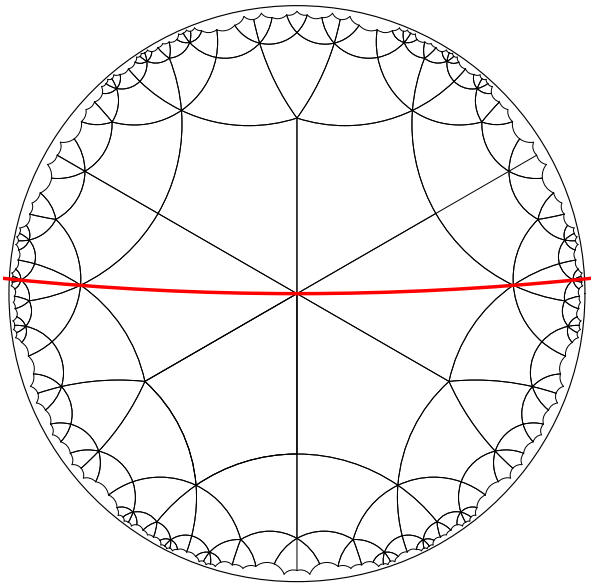

Figure 10: The kite tessellation and a backbone line equidistant curve for a $(4, 5, 3)$ pattern.

Figure 11 shows the $(5, 3, 3)$ pattern of Figure 4 translated so that it is "nose-centered" like the *Circle Limit III* pattern of Figure 6. In each of patterns of Figures 4 and 12, the backbone lines form a Euclidean equilateral triangle. All four of these patterns show that the backbone lines are not hyperbolic lines, since hyperbolic lines are represented by straight Euclidean lines if and only if they pass through the center of the bounding circle.

5. Conclusions and Future Work

For any (p, q, r) pattern, we have shown a calculation that computes the angle ω an equidistant "backbone" curve makes with the bounding circle. Another unanticipated outcome was to figure out how to transform a fin-centered *Circle Limit III* pattern to a nose-centered pattern, as was done in Figures 6 and 11.

However, there is still work to be done. I would certainly like to know if it is possible to simplify the calculation above down to a single formula as was done for the special $(p, 3, 3)$ that was treated in my 2006 Bridges paper [4]. It would also be useful to be able to transform one (p, q, r) pattern to another one with different values of p, q, and r. A seemingly difficult problem is to automate the process of coloring a (p, q, r) pattern so that it has the same color along any line of fish and adheres to the map-coloring principle that adjacent fish have different colors. Currently I determine colorings "by hand", and although it may be

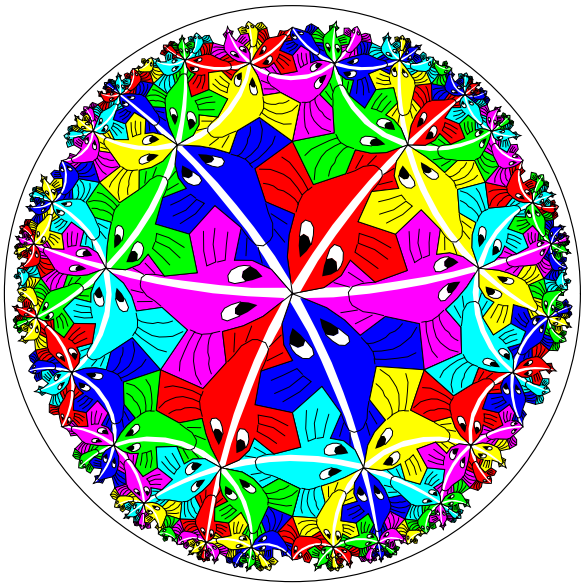

Figure 11: A nose-centered version of the (5,3,3) pattern.

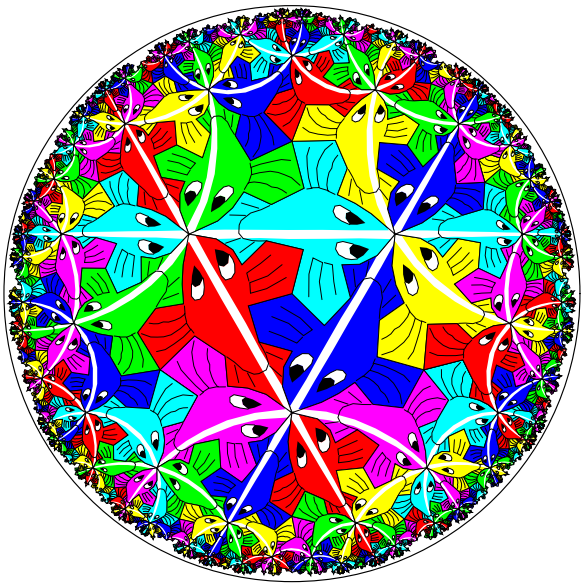

Figure 12: A (3,5,3) pattern related to our patterns of Figures 4 and 11.

possible to program symmetric colorings of any repeating pattern, the requirement that fish along a backbone line be the same color adds an extra degree of difficulty to coloring (p, q, r) patterns.

Acknowledgments

I would like to thank Lisa Fitzpatrick and the staff of the Visualization and Digital Imaging Lab (VDIL) at the University of Minnesota Duluth.

References

[1] Anonymous, *On the Cover,* Mathematical Intelligencer, **18**, No. 4 (1996), p. 1.

[2] H.S.M. Coxeter, *The Non-Euclidean Symmetry of Escher's Picture 'Circle Limit III',* Leonardo, **12** (1979), pp. 19–25.

[3] H.S.M. Coxeter. *The trigonometry of Escher's woodcut "Circle Limit III",* Mathematical Intelligencer, **18**, No. 4 (1996), pp. 42–46. This his been reprinted by the American Mathematical Society at: `http://www.ams.org/featurecolumn/archive/circle_limit_iii.html` and also in *M.C. Escher's Legacy: A Centennial Celebration,* D. Schattschneider and M. Emmer editors, Springer Verlag, New York, 2003, pp. 297–304.

[4] D. Dunham, *More "Circle Limit III" Patterns,* in Bridges London: Mathematical Connections in Art, Music, and Science, (eds. Reza Sarhangi and John Sharp), London, UK, 2006, pp. 451–458, 2006.

[5] M. Greenberg, *Euclidean & Non-Euclidean Geometry, Third Edition: Development and History,* 3nd Ed., W. H. Freeman, Inc., New York, 1993. ISBN 0716724464

[6] David Hilbert, Über Flächen von konstanter gausscher Krümmung, *Transactions of the American Mathematical Society,* pp. 87–99, 1901.